Proyecto Fin de Máster

Optimization of Full Bridge topology with triangular current for avionic applications

Yann Emmanuel Bouvier Rescalvo

Máster en Electrónica Industrial

Universidad Politécnica de Madrid

Centro de Electrónica Industrial

Escuela Técnica Superior de Ingenieros Industriales

Departamento de Automática, Ingeniería Electrónica e Informática Industrial

September, 2014

Universidad Politécnica de Madrid

Centro de Electrónica Industrial

Escuela Técnica Superior de Ingenieros Industriales

Departamento de Automática, Ingeniería Electrónica e Informática Industrial

Máster en Electrónica Industrial

Optimization of Full Bridge topology with triangular current for avionic applications

Author: Yann Emmanuel Bouvier Rescalvo

Directores: Pedro Alou Cervera

Miroslav Vasić

September, 2014

Proyecto Fin de Máster

Acknowledgments

To my tutors, Pedro and Miroslav, and also Jesús for all of their knowledge shared and patience with me.

To my parents, for their love and for supporting me in everything.

To Sisi, Uros and Marcelo for all of their help and support in all of the projects.

To Ana for helping me in the decision to start this Master. I never would have done it without your support.

To all of the CEI and Master companions for all the good times and the great atmosphere

A very special thanks to someone very special; Mavi, for these awesome four years and the good times shared.

Contents

Introduction

There is a strong tendency in aircraft designs towards a More Electric aircraft (MEA). This concept is the consequence of the substitution hydraulic, pneumatic and mechanical systems and sub-systems with electrical equivalents. This results in an ever increasing demand for the aircraft's power requirements. Drivers of weight and cost reduction are also taken into consideration for this new design philosophy. The ultimate goal of this philosophy is to distribute only electrical power across the airframe. This comes at the cost of increasing the power of electronic converters, this poses the challenge to design and build such converters with the least amount of weight and volume.

To cope with this increase of electrical power, in the area of military aircraft, the traditional voltage levels of 28VDC has evolved to 270VDC. One of the main benefits of this high voltage is that the current levels are 10 times lower than with conventional low voltage. Therefore, it is possible to reduce the amount of copper used for wires and by that reduce volume and also weight, either of them critical in aircraft design. To supply power in DC voltage it is usually required to have an AC-DC rectifier, as the primary generators in a aircraft work with alternating current.

In order to have a successful and efficient design for such a demanding application, there is the need to use state of the art power topologies, components and control methods. The focus of the design for this type of converters is usually the reduction of weight and volume at the highest efficiency possible, the cost is by consequence not a primary concern. The most challenging components for this type of converters are usually the magnetic components, as they are the biggest in both volume and weight, high frequency effects are also of big importance and they should be analyzed carefully in order to achieve an optimum design. Because of the high power required, switching devices are also a problem not only because of high conduction losses but also because of the increase effect of switching losses. Additionally, this type of converter are typically required to have galvanic isolation, high power factor, low current THD and good dynamic control of the supply voltage.

Project objectives and topology

The present Master work formed a part of the research project that originated from the collaboration of the Center of Industrial Electronics from the Technical University of Madrid, Indra and Airbus Defense and Space, two companies involved in the design and implementation of electronic equipment and software for aircraft applications.

This project's main objective is to design and validate a prototype for a 45 kW DC-DC converter with restrictive dynamics for an aircraft application. This converter is part of a bigger system, an AC-DC rectifier consisting of three main parts.

- **EMI filter** at the input to cope with the regulations concerning harmonic distortions.
- **AC-DC rectifier** to convert the alternating current to direct current and also regulate the power factor of the AC input.
- **DC-DC converter** to adjust the output voltage to the level required and improve the dynamic response of the system to load steps.

The requirements for this system are the following:

- **Isolation**: It is needed for the converter to be isolated, this can be achieved in any of the stages but usually the isolation is in the DC-DC converter, as it is typically a full-bridge topology, with transformer.
- **Limited volume and weight:** This system is designed for an aircraft application and so there are heavy restrictions in the total amount of weight and volume for it.
- **Parallelizing:** The system needs to be able to be parallelized; this entails some kind of current loop in the system.
- **Robustness and cost:** The devices used in this system need to be of military rating and also a digital control is required in order to decrease the cost and increase the robustness
- **Dynamic requirements:** The system needs to be able to withstand the transient of load step previously defined.

I. Specifications

As explained in previous sections, this converter is for a military aircraft application, the specifications are defined in the following table.

Table 1
DC-DC converter speficication

Input Voltage	**Vin**	450 V
Output Voltage	**Vout**	270 V
Output Power	**Pout**	45 kW
Temperature range	**T**	-55º to +85º
System target weight	**W**	10 kg

I.1 Input voltage

This converter is actually part of a bigger system consisting in a rectifier stage in cascade with this DC/DC converter. The value of the input voltage is not in principle fixed by any specification but it influences voltage ratings of the devices used both in a boost type rectifier and the primary devices for the dc-dc converter. This DC bus voltage is also very influenced by the topology of the rectifier (boost type or buck type). A trade-of has been analyzed between the advantages and disadvantages of the DC bus voltage for both the rectifier stage and the dc-dc converter stage. The final value for this dc bus voltage is chosen at 450V. Taking into account the military derating (30%) necessary for this application, the input devices for this converter should have a breakdown voltage of at least 600V.

I.2 Output voltage

The output voltage is fixed by specification at 270V as the new DC Voltage for aircraft applications, as explained in the More Electric Aircraft section. Taking into account the military derating, the secondary devices should be selected with a voltage breakdown of at least 400V

I.3 Temperature range

The temperature range is the military temperature range. This should influence mostly in the selection of components, not only for the power stage but also for the entire component in the control and sensor boards.

I.4 Target weight

The target weight is actually an estimation; the target weight is defined for the overall system (AC-DC rectifier included) at 45kg. The AC/DC rectifier is usually much bigger and with more weight than the DC/DC converter. So it can be expected of the DC-DC converter to not exceed 8kg (without heat sink)

II. Comparison of state of the art topologies

The state of the art for isolated DC/DC topologies for high power and efficiency is always related to full-bridge topologies or similar. In this chapter, these topologies are going to be presented and compared.

1. Full-bridge phase shifted converter

The full-bridge phase-shift is a robust converter that has high power density and efficiency [2]. However, this topology usually works in continuous conduction mode so primary side transistors are always turned on with hard transitions. Even though this topology can achieve zero voltage switching at the turn-on, this gives four hard transitions per cycle.

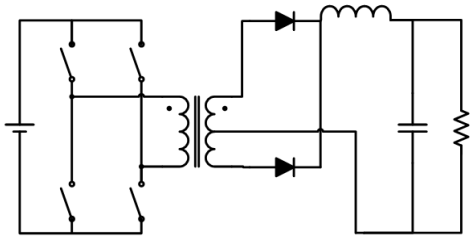

Figure 1: Full bridge phase shifted

The diodes on the secondary side are turned off by applying negative voltage between its terminals and in order to avoid power losses due to reverse recovery, Schottkey diodes should be used. Having in mind the high voltage that the secondary diodes have to withstand, the only solution for them is the Silicon Carbide (SiC) diodes that have high conduction losses and penalizes the overall efficiency.

This topology also needs a center-tapped transformer, which is more complex to build than a typical transformer and also there is the need for a external inductor. This results in more volume and weight for the overall system.

2. Dual active bridge

This topology uses two sets of full bridges to achieve a bidirectional converter. This converter can also have a triangular modulation of the current and can have only one magnetic component if the leakage is used as the primary inductor. The bidirectional

behavior is not needed in our design and it is needed to have 8 controllable switches which is additional complexity in the design.

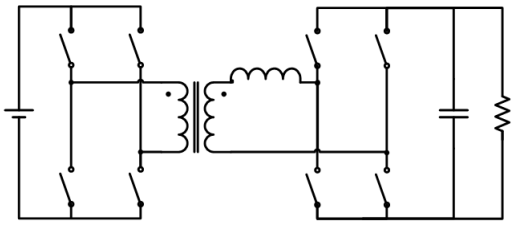

Figure 2: Dual active bridge

3. Dual active bridge series resonant converter

The Bidirectional Dual Active Bridge Series Resonant Converter (DAB SRC) [2] is a type of dual active bridge that attenuates switching losses by the use of a resonant capacitor in series with the leakage inductance of the transformer. The main advantage of this topology is the ZVS in all switches at cost of a more complicated control. Also the output voltage cannot be controlled it is always proportional to the input voltage. Another advantage of this topology is the bidirectional power transfer, but in the case of our application it is not useful.

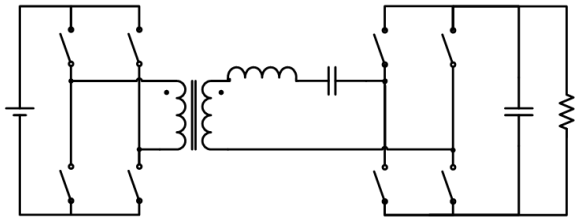

Figure 3: Dual active bridge series resonant

However for this high power application, this kind of resonating converter has never been implemented. This is probably the most efficient of the full-bridge converter because it can have the fewer amounts of losses by eliminating completely the switching losses in all devices with the resonance. However it does not have a controllable output voltage, which in principle the rectifier stage could take care of the control, but if dynamic responses are necessary it is best for the DC-DC part to have a control loop to increase the bandwidth and increase the dynamic response of the converter to load steps.

4. Triangular current waveform full-bridge

The Triangular current waveform full-bridge is a topology that uses the leakage inductance of the transformer to achieve a triangular current waveform and has ZCS in the primary switches [3]. This topology is a special case of the dual active bridge

with diode bridge at the secondary, losing by this the bidirectionality. It also minimizes the reverse recovery effect in the secondary bridge.

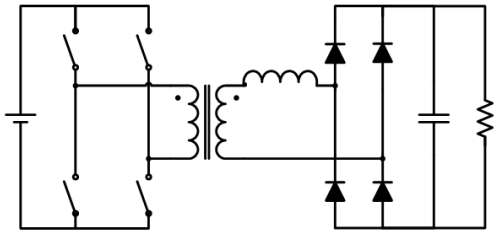

Figure 4: Triangular current waveform full-bridge

The main advantages of the triangular full-bridge are the soft transitions in the diode bridge and in the primary switches, and that it only needs one magnetic component, given that the leakage inductance can be used as the inductor of the converter. Due to the fact that the leakage inductance of the transform is used to shape the primary current, and that this current has high ripple, high capacitance is needed at the output. This capacitance can occupy significant volume and it is a drawback of this topology.

This is the topology chosen to be validated for this application. It has the most promising efficiency and robustness without losing the control of the output voltage and its able to be parallelize with ease and it can handle the dynamic requirement.

III. Triangular current full-bridge topology

The triangular current full-bridge has three main components:

- **Transistor bridge:** Located in the primary of the transformer, in the same way as a conventional full-bridge topology
- **Transformer:** This transformer also works as the main inductor of the topology, using the leakage inductance.
- **Diode bridge:** At the secondary of the transformer and connected to the output, it rectifies the alternating triangular current of the transformer to deliver direct voltage to the load.

Generally, capacitors are added to the output of the system to attenuate the ripple in the voltage. Input capacitors can also be added in order to ensure stability of the input voltage.

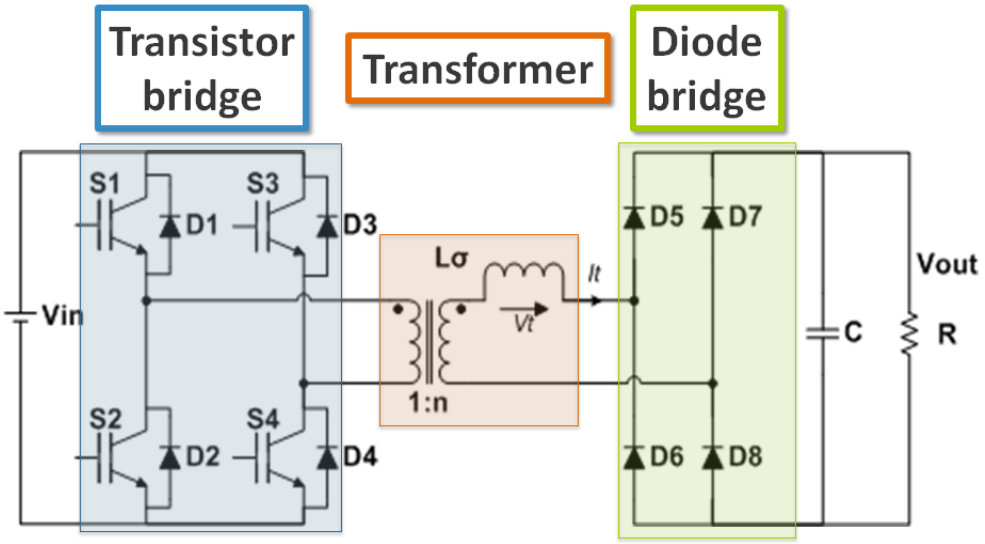

Figure 5: Triangular current full-bridge detailed schematic

The triangular current full-bridge has a number of advantages:

- **Soft transitions** in all devices except for one hard switching per cycle in the high-side primary devices.
- **Only one magnetic component** is needed for this topology, as the transformer act both as transformer and main inductor using the leakage inductance. This can reduce both the volume and weight of the system.

- **Easy control:** This topology has a very easy control. It can be controlled with a single PWM signal. Transistors in one leg are complementary and from leg to leg they have a 180º constant phase shift.

This topology also has some disadvantages, mainly:

- **High RMS currents:** The discontinuous conduction mode is forcing the converter to work with high RMS currents in comparison to other continuous conduction mode topologies. This cause more conduction losses overall and also more losses in capacitors that need to handle a bigger current ripple.
- **Leakage inductance:** As any converter that is designed around a parasitic parameter, it has the problem of accuracy of estimation of that parameter. Also the need for leakage in the transformer forces a non-optimal design for the windings, preventing the use of common methods like interleaving to be used.

Principle of operation

Figure 6 shows the current of the transformer secondary and its voltage. A detailed explanation of the modulation is presented next:

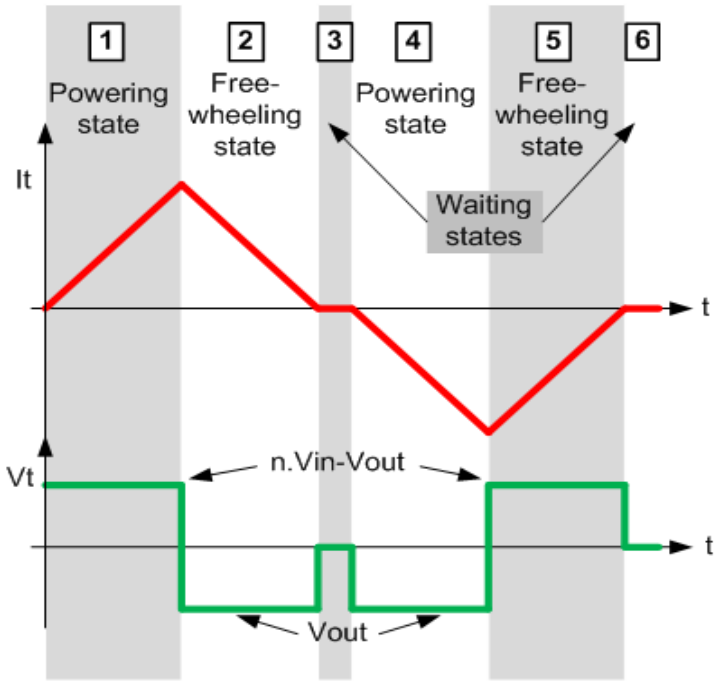

Figure 6: Triangular full-bridge switching cycle

1) First Powering state, from t0 to t1, S1 and S4 switches are turned on. The input voltage is applied to the primary of the transformer and the output voltage to the secondary. The current rises linearly due to the leakage inductance of the transformer. In secondary side, diodes D5 and D9 are conducting the output current. The slope of the current can be calculated with the following equation.

$$\frac{\Delta I}{\Delta t} = \frac{(n \cdot V_{IN} - V_{OUT})}{L_\sigma} \quad (1)$$

2) First freewheeling state, from t1 to t2, S1 is turned off and after a dead-time S2 is turned on. The current flows through the parallel diode D2 and S4. The voltage applied to the primary is zero and the output voltage in the secondary side, so the current drops linearly and the slope is calculated with this equation.

$$\frac{\Delta I}{\Delta t} = \frac{-V_{OUT}}{L_\sigma} \quad (2)$$

3) First waiting state, from t2 to t3, the current has finally reached zero. A small sinusoidal current due to the resonance of the leakage inductance and diode parasitic capacitance can be observed during this time interval.

4) Second powering state, from t3 to t4, S3 and S2 are turned on. The current decreases to negative values. This stage is equivalent to the t0 to t1 stage. In the secondary side, D6 and D7 are conducting the output current.

5) Second freewheeling state, from t4 to t5, S3 is turned off and S2 is turned on, the current flows through D4 and S2.

6) Second waiting state, from t5 to t6, the current in the transformer is zero and the next switching cycle can begin.

The principal advantage of this topology is the soft switching of the devices. There are only two hard switching in both high-side transistors in a switching cycle, at t1 for S1 and at t3 for S3. Also the diodes in the secondary side are always turn on and off softly, reducing the problem of reverse recovery in those devices. To achieve ZCS in the primary transistors it is fundamental to avoid continuous conduction. This can be done with an accurate control of the slopes in the triangular current. The equations (1) and (2) define the slopes for the triangle waveform. The input voltage Vin, the turn's ratio n and the leakage inductance Lσ are critical parameters in the design of this topology.

In order to avoid continuous conduction mode the parameters have to comply with the following equation:

$$\frac{n \cdot V_{IN}}{V_{OUT}} \cdot \frac{L_\sigma \cdot \Delta I}{(n \cdot V_{IN} - V_{OUT})} \leq \frac{T_S}{2} \tag{3}$$

If the triangle shape is symmetrical, then, we have an additional equation fixing the value for n. The triangle will be symmetrical if the slopes are the same, so equations (1) and (2) need to be equaled.

$$\frac{V_{OUT}}{L_\sigma} = \frac{(n \cdot V_{IN} - V_{OUT})}{L_\sigma} \Leftrightarrow n = \frac{2 \cdot V_{OUT}}{V_{IN}} = 1.2 \tag{4}$$

In one half of the switching cycle the current has to rise and fall in time. A good design solution, to take into account transient and load steps is to give some amount of wait-time (t3 to t4 and t5 to t6) in order to have a safe margin and never reach the continuous conduction mode. It is important to avoid the continuous conduction mode, not only to achieve zero current switching in the devices but also because stability problems can arise as a consequence.

Since the high-side devices are the ones having hard switching a modulation of the freewheeling state always in the low side device is needed in order to balance the power losses of the transistors.

Design and losses calculation

To validate the triangular current full-bridge topology, the building of a prototype is needed. Before that, a process of design and estimation is necessary.

All of the devices must meet with military standards as this prototype is for a military aircraft application. The derating is always of 30% above for all voltage breakdowns and maximum temperatures.

I. Semiconductors

I.1 Primary devices

The primary devices are blocking a voltage equal to the DC bus voltage 450V. Applying the military derating, devices of at least 600V rating are needed for this prototype.

For the transistors in the primary side of the converter either MOSFET or IGBT can be chosen. MOSFET can be used at higher frequencies than IGBT but this increases also the power losses by switching effects. IGBT's can handle better high current and less of them in parallel are needed to withstand currents of that magnitude.

For the comparison of MOSFET and IGBT for this topology one IGBT and one MOSFET are chosen to be compared: APTLGT400A608G for the IGBT and APT80M60J for the MOSFET.

Table 2
Comparison of MOSFET and IGBT

	Power losses	Nº of devices in parallel
MOSFET	1536 W	4
IGBT	519 W	1

Analyzing the results, it is obvious that IGBT's have a clear advantage in this topology with fewer losses and also less amount of devices in parallel

I.1.1.1 Conduction losses

The conduction losses for an IGBT device are determined by the following equation:

$$P_{cond\_IGBT} = V_{CE} + R_c \cdot I_{RMS}^2 \quad (5)$$

Where Vce and Rc are values of the Collector-Emitter voltage drop and resistance of the IGBT that can be obtained with the information in the datasheet. The following figure is the output characteristic, where this information can be derived.

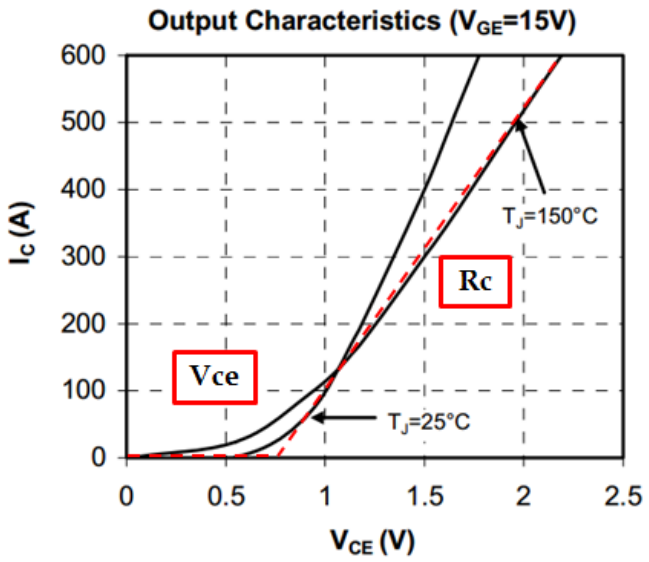

Figure 7: Output characteristic of APTLGT400A608G IGBT

From the slope of the output characteristic the value of Rc can be calculated. The value of Vce is the voltage at which the current reaches zero, or an approximation.

For the IGBT modules APTLGT400A608G the values are the following:

- $V_{CE} = 0.6\,V$
- $R_c(85℃) = 3.65\,m\Omega$

I.1.1.2 Switching losses

As explained in the topology chapter, the high side primary devices have a hard turn off. The input voltage and frequency are constant in this topology, so the peak current of the triangular modulation is the critical factor for the amount of switching losses.

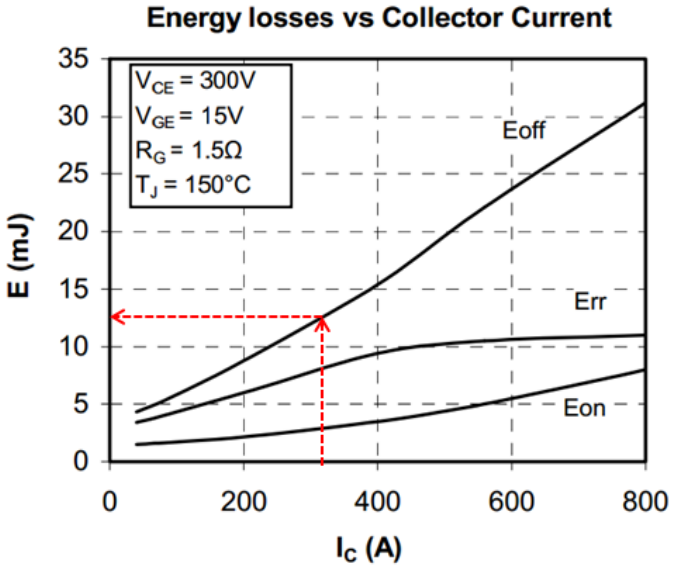

Figure 8: Energy losses vc. Collector current of APTLGT400A608G IGBT

$$P_{\text{Switching\_}IGBT} = E_{off}(I_c) \cdot \frac{450}{300} \cdot f_{sw} \tag{6}$$

The value of Ic for this topology is the peak of the triangular current, at which the transistors are turned off. The value of this current peak is highly dependent on the leakage and modulation of the topology.

In Figure 6 the current of both high-side and low-side IGBT of the simulation results are plotted. As it was explained in the topology overview, during the freewheeling state the low side transistors are conducting the current until it reaches zero and the wait time starts.

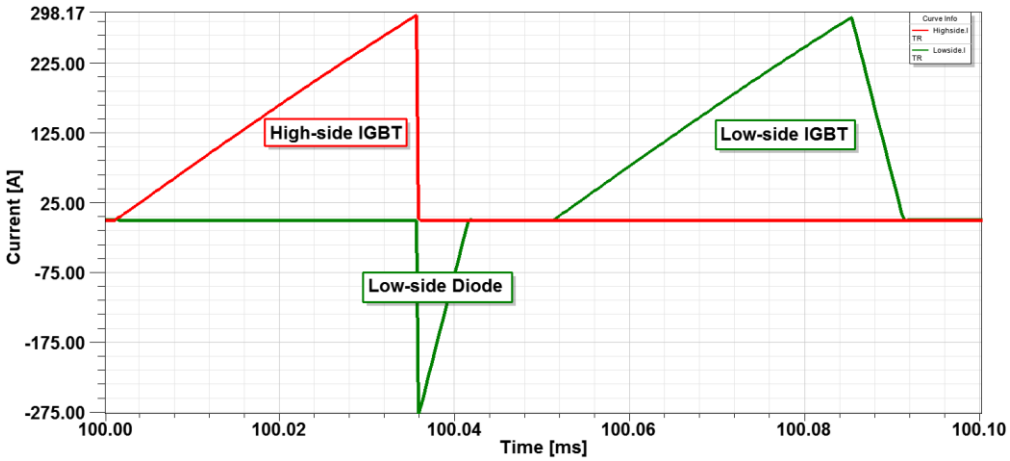

Figure 9: Primary IGBT current simulation

However, in the case of IGBT, which does not have bidirectional conduction, the antiparallel diode is conducting that current. This needs to be taken into account for the calculation of losses; the antiparallel diode can have more losses than the IGBT.

I.2 Secondary devices

For the semiconductors in the secondary part of this topology diodes can be used as there is no need for any bidirectionality. Transistors can be used if there is the need to decrease the amount of conduction losses, at the cost of increasing the complexity for the control scheme. For this design it is preferable to used diodes for added robustness.

The current that is handled by those devices is showed in the following figure.

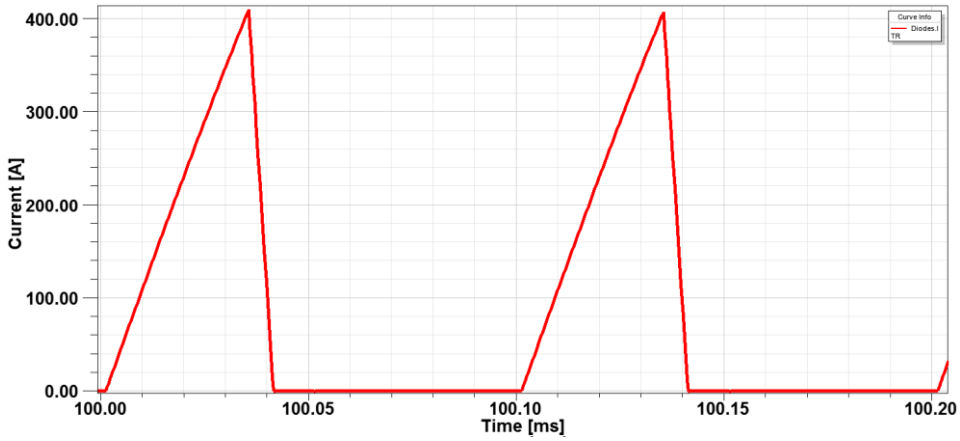

Figure 10: Secondary diodes current simulation

The diodes chosen for this topology are MEE 300-06DA from Ixis. They don't need to have very good switching characteristics because both turn on and off are soft, as it can be seen in the figure

Conduction losses for these diodes can be calculated with the following equation

$$P_{cond\_diodes} = V_f + R_d \cdot I^2_{RMS_{diodes}} \quad (7)$$

Where the values for Vf and Rd are the forward voltage of the diode and the resistance, they can be easily checked in the manufacturer's datasheet.

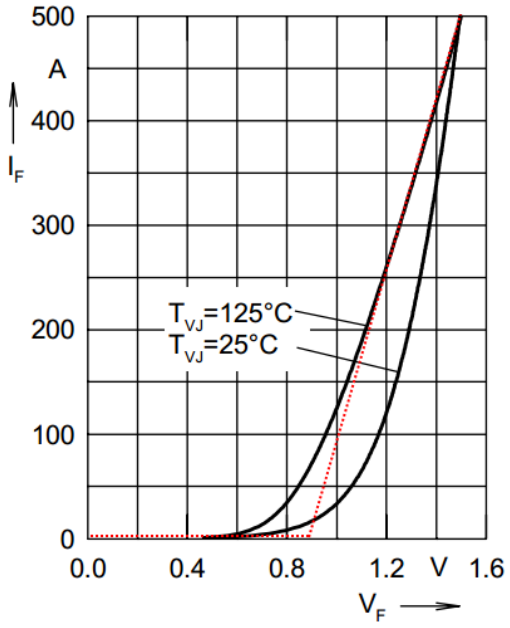

Figure 11: MEE 300-06DA Diode characteristic

For the diodes modules MEE 300-06DA the values are the following:

- $V_{CE}(85℃) = 0.85\ V$
- $R_c(85℃) = 1.36\ m\Omega$

II. Transformer

The transformer is a critical component in this topology. The value of the leakage inductance is what makes this topology possible and avoids the use of an additional inductor, reducing considerably the power losses and also reducing substantially the volume and weight of the converter. However, the need to have such high value for the leakage inductance can increase the losses in this component and increase the complexity of the design, as it is going to be explained in the following section.

II.1 Nanocrystalline material

This prototype is designed for a very demanding application, combining both high power with low volume and weight. The selection of the core material for the transformer is critical. For high power density design nanocrystalline material has the best performance in comparison with conventional ferrites or even amorphous materials.

Nanocrystalline material is a alloy based on Iron (Fe) with Silicon (Si) and boron (B) with Niobium (Nb) and Copper (Cu) additives. This material has a crystalline structure at the nanoscale. The average grain diameter is between 10 and 40 nanometers.

This material has very good magnetic behaviour in comparison to typical ferrites.

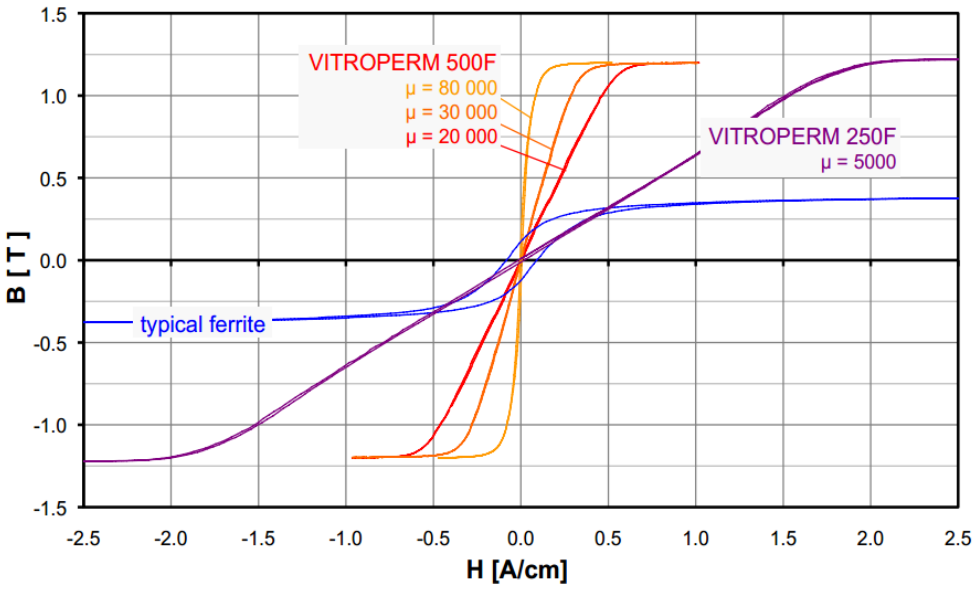

Figure 12: Vitroperm 500F B/H magnetization curve

As can be seen in the figure above, this material has a very high saturation flux (1,4T) and also a very high and linear permeability. The hysteresis cycle is very narrow in this material, which lowers significantly the amount of core losses per unit of volume.

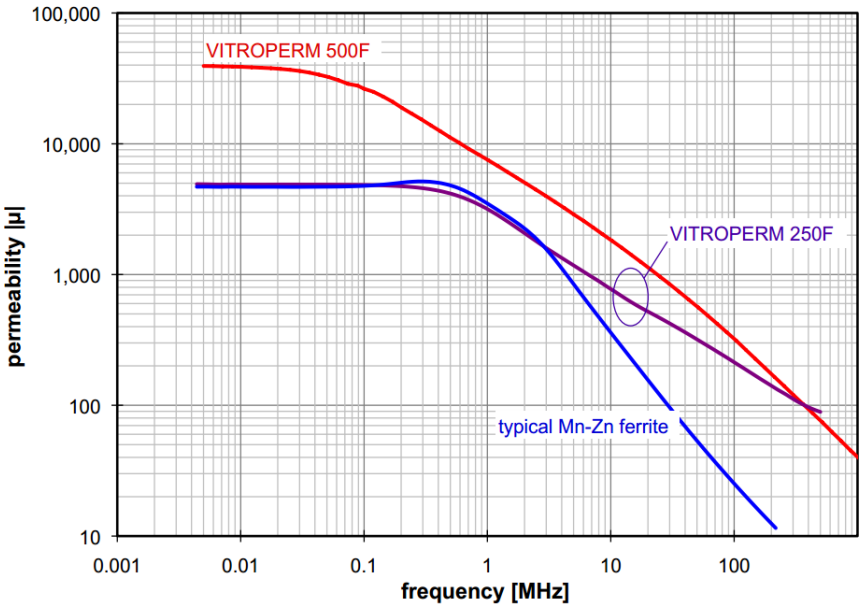

Figure 13: Vitroperm 500F permeability vs. frequency

This material has very good behaviour at the frequency range at which the converter works (10 kHz), this can be seen in the figure above.

II.2 Improved Steinmetz equation for core losses

For the calculation of the core loses the Steinmetz equation is usually used for the calculation of the core losses by unit of volume.

$$P_V = k \cdot f^{\alpha} \cdot \hat{B}^{\beta} \tag{8}$$

However this equation is only completely valid for sinusoidal current. To estimate the core losses accurately for this topology the improved Steinmetz equation is needed. This improved equation takes into account the derivative of the B field and it uses the same parameters alpha and beta from the original Steinmetz equation, those parameters are usually given by magnetic manufacturers in the datasheets.

$$P_V = \frac{1}{T}\int_0^T k_i \left|\frac{dB}{dt}\right|^{\alpha} (\Delta B)^{\beta-\alpha} dt \tag{9}$$

Where ΔB is the peak to peak flux density and

$$k_i = \frac{k}{(2\pi)^{\alpha-1} \int_0^{2\pi} k_i |cos\ \theta|^{\alpha}\ 2^{\beta-\alpha} d\theta} \tag{10}$$

Where k, α, and β are the same parameters as used in the Steinmetz equation.

The shape of the magnetizing current through the transformer is showed in the following figure

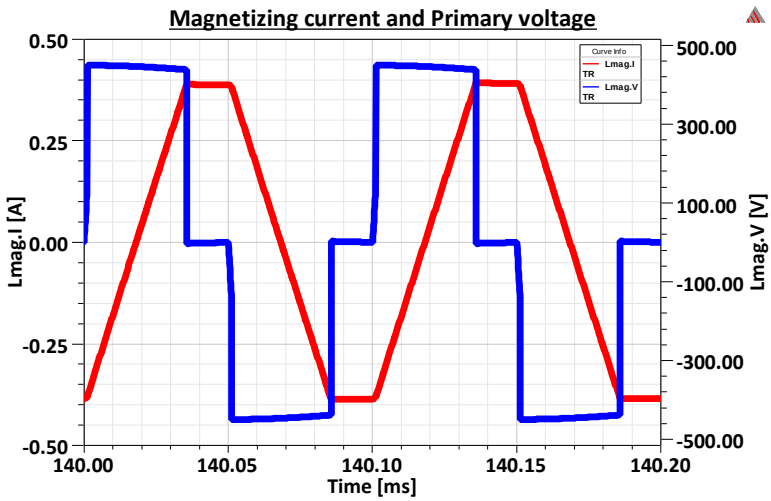

Figure 14: Magnetizing current and primary voltage of the transformer

It has to be noted that for the calculation of the improved Steinmetz equation the parts where the current hence the flux B is constant have a null contribution to the integral. And for the rest of the shape of the current the derivative |dB/dt| has a constant value so the calculation of the integral is straight-forward.

II.3 Copper losses and skin effect

For the calculation of the copper losses in the transformer the high frequency effects are relevant and need to be added to the calculation. The value of Rdc of the transformer is not good enough for the calculation. It is then required to take into account up to the 5th harmonic of the triangular current. For that the copper losses are calculated using the following equation.

$$P_{copper} = R_{10kHz} \cdot I_{10kHz}^2 + R_{30kHz} \cdot I_{30kHz}^2 + R_{50kHz} \cdot I_{50kHz}^2 \tag{11}$$

The value of the resistance for different frequencies must be obtained by finite element analysis of the transformer with foils, as it is going to be explained later in this chapter.

The frequency of this prototype for this converter is going to be in the order of magnitude of 10 kHz but with the triangular shape of the current adds some harmonic content. It can be calculated that the harmonic content is relevant for losses calculation and skin effect consideration until the 5th harmonic, 50 kHz. In order to minimize the skin effect and keep the AC resistance of the windings as low as possible, it should be necessary to use Litz wire. However, the power density of this converter is very high and it is impossible to find Litz wire for that amount of power, for the use of copper foils or pletinas. The thickness of the copper foil must be twice the skin depth of copper at 50 kHz, which is 2*0.3 = 0.6 (mm) and it is calculated with the following equation.

$$\delta_{copper} = \sqrt{\frac{\rho_{copper}}{\pi \cdot f \cdot \mu_{copper}}} \tag{12}$$

Where ρ_{copper} is the resistivity of copper in Ω.m, f is the frequency in Hertz, μ_{copper} is the absolute magnetic permeability of copper $\mu_{copper} = \mu_o = 4\pi.10\text{-}7$ H/m

II.4 Leakage inductance and AC resistance estimation and realization

As explained previously in this work, the leakage inductance of the transformer needs to be accurately calculated because it is a critical variable in the design of the converter. Once the values of the input and output voltages are set and the turn's ratio of the transformer and switching frequency of the converter are fixed there is a maximum value for the leakage inductance which is fixed by the following equation. Values lower than this maximum will end up giving more time for the wait phase of the switching cycle. This can be needed in order to avoid continuous conduction mode in transients, but it also can be coped with a slight decrease of the switching frequency

For this topology a value between 3μH and 10μH is needed, with values in that range, the optimum switching frequency should be close to 10 kHz, which is a value acceptable to driving IGBT's. To achieve such a high value of the leakage inductance in a transformer there is the need to have a big H field between the windings. This can cause problems in the distribution of current by proximity effect and so the relative position of the windings must be the correct to attenuate the proximity effect influence in the distribution of current through the conductors.

In order to obtain a high leakage inductance it is needed to have a less than optimal coupling of the windings which is detrimental in the point of view of optimizing losses. Interleaving is a very common method to decrease the AC resistance of the

winding and also decrease the usually unwanted leakage inductance. However this is not the case for this topology, so interleaving should not be used.

The use of copper foils can have an impact in the way the windings can fit in the window of the transformer. The leakage inductance is strongly dependent on the windings position and geometry, the use of copper foil has a beneficial impact on these as they are more accurately positioned than conventional wires.

In a U shape core there are 3 main ways to wind without interleaving, showed in the figure below.

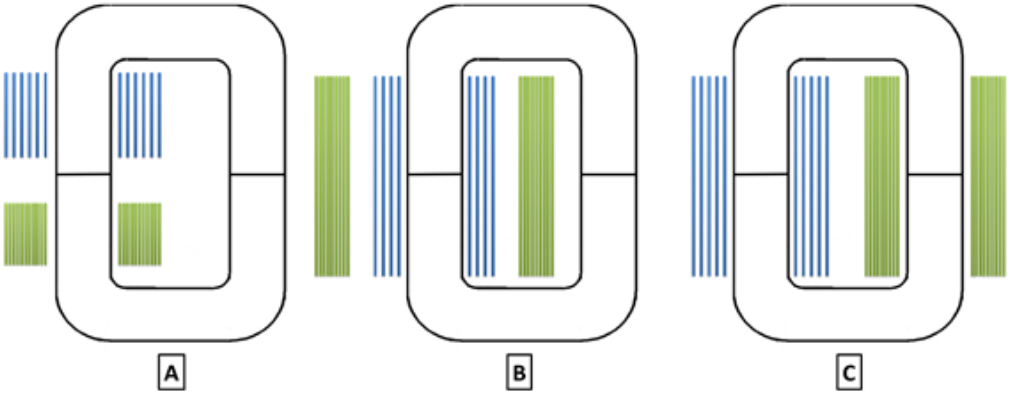

Figure 15: Three ways to wind a transformer with foils without interleaving

These transformer's winding configurations are very different between each other in terms of AC resistance and leakage inductance and there is the need to analyze the effect of each one in order to know which the most efficient solution for this topology.

II.4.1.1 Type A Transformer

This configuration was the first to be tried in real transformer for the prototype, for the capability to estimate the leakage inductance with ease managing the distance between windings. None the less, some difficulties arise when the AC resistance is estimated by finite element analysis, which affects the power losses. In the next figure, the leakage flux path can be seen.

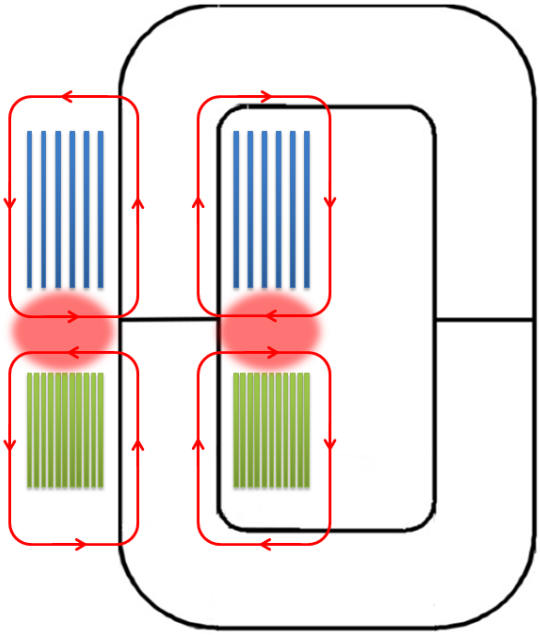

Figure 16: Type A transformer flux path B and magnetic field H concentration

If the magnetic H field is also taken into account, it will stronger where the windings are the closest, as it can be seen in Figure 16 in the red shaded area. This concentration of magnetic H field near the windings causes proximity effect in the copper foils near it. In this configuration, the proximity effect will force the current to flow closer to the concentration of magnetic field, wasting the whole width of the copper foil and increasing the AC resistance.

II.4.1.2 Type B Transformer

This configuration is better than the last one. There is an improvement in the AC resistance, so this transformer can achieve better efficiency. However, this configuration has a better coupling than the others and it will entail a smaller leakage inductance, which in our topology is going to be detrimental.

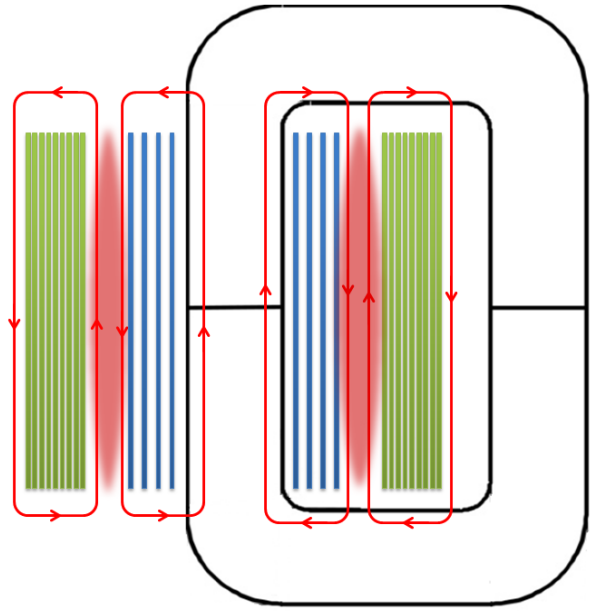

Figure 17: Type B transformer flux path B and magnetic field H concentration

For this configuration, the proximity effect is also present but it will only affect the two foils closer to the concentration of H field. The width of the foils will not be wasted because of it, so an improvement in the AC resistance must be seen.

II.4.1.3 Type C Transformer

This configuration is similar to the type B, the only difference is the windings are in separate legs of the U core. It is expected to have a bigger leakage inductance because the coupling is worse than with both windings in one single leg.

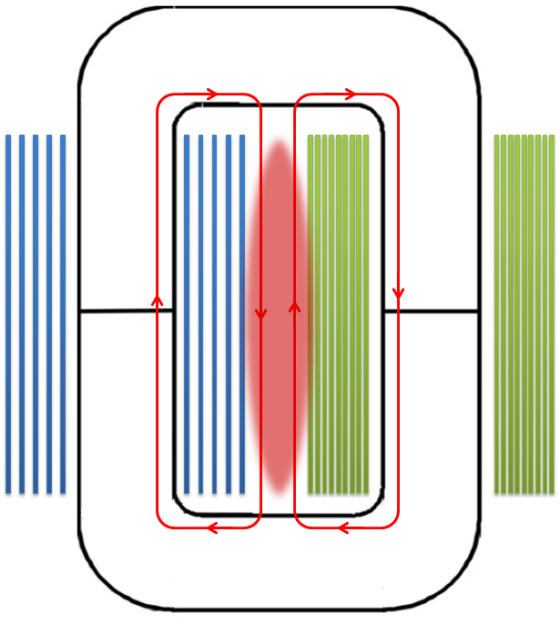

Figure 18: Type C transformer flux path B and magnetic field H concentration

In this configuration of windings the concentration of H field is very much localized and it will affect in a smaller amount the AC resistance than the other configurations. It should be expected for this topology a significant decrease in AC resistance. Another benefit of this configuration is the higher surface area to be linked with the heat sink, which will increase the efficiency of the heat sink and allow for better cooling of the transformer.

II.4.1.4 Comparison of transformer's configurations

The three configurations for the winding of the transformer need to be compared in order to find the optimum one, not only in terms of transformer losses but also in terms of overall efficiency. The transformer's leakage inductance is a critical variable in the modulation and shape of the current for the triangular current full-bridge topology, so the design of the transformer is critical to the whole system.

An estimation of the AC resistances of the windings is necessary for the correct estimation of the copper losses in the transformer. As it has been explained before, the shape of the current contains harmonics relevant up to 50 kHz which means that the value for the AC resistance (variable in frequency) is also very relevant to the estimation of losses. In the next figure the values of AC resistance for each configuration can be seen.

To estimate the values for the AC resistance of the transformers and also the leakage inductance a finite element analysis is needed. For this purpose the software PEMag 7.1 is used.

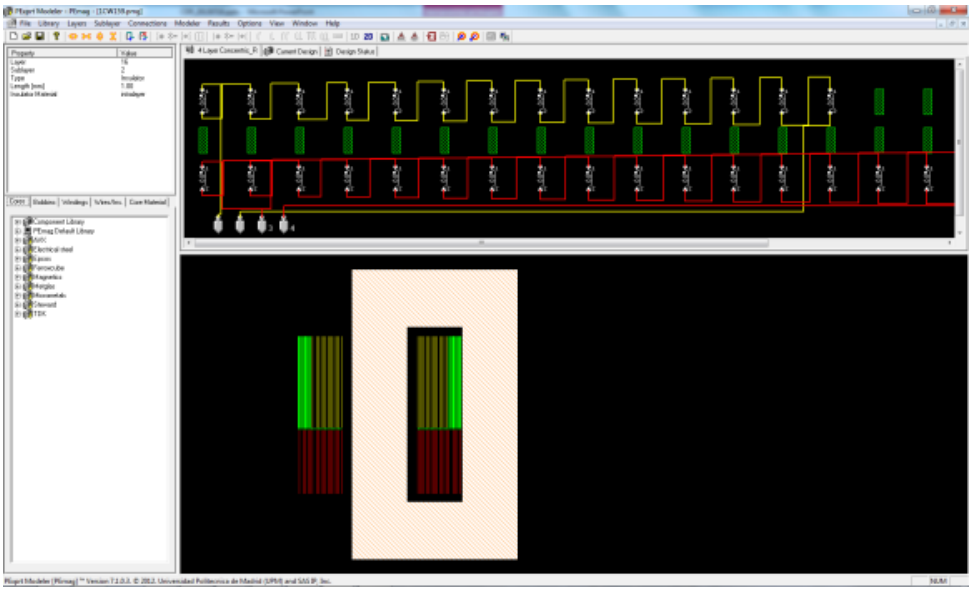

Figure 19: PEMag 7.1 software environment

In the program PEMag 7.1 the position, shape and material of the windings is possible to define. It also takes into account the material and shape of the core. With this program the leakage inductance can be estimated as well as the AC resistance for a range of frequencies and also the capacitive effect of the foils.

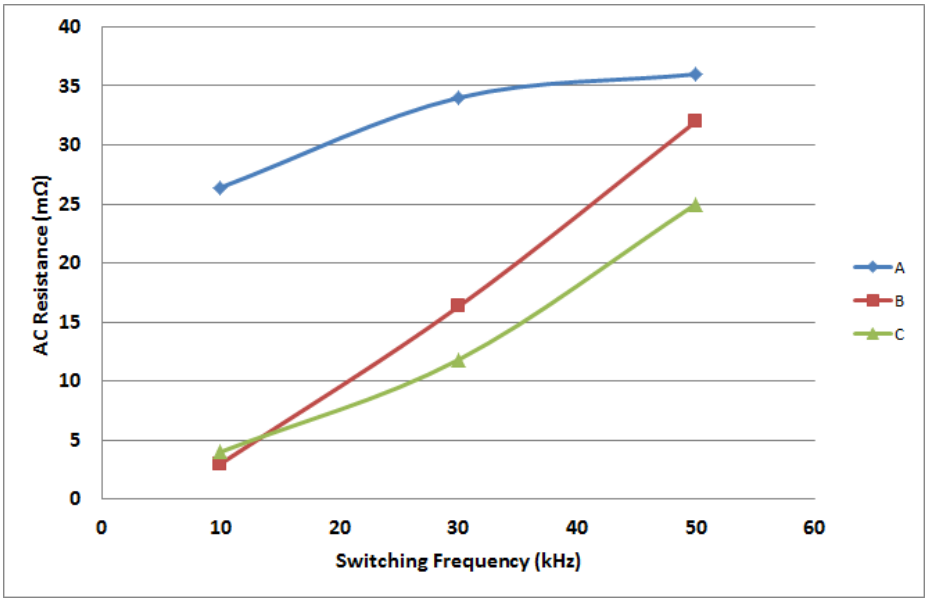

Figure 20: AC resistance of each type of transformer vs. switching frequency

In the figure above, it can be observed that, as explained, the values for type A transformer are bigger in all of the frequency range. The AC resistance for the transformers of types B and C are quite similar to each other with type C been little below than type B at higher frequencies.

The next table shows the leakage inductance for each of the configuration.

Table 3
Leakage inductance for each transformer type

	Type A	Type B	Type C
Leakage Inductance	3.5 µH	1 µH	4 µH

As expected the value of leakage inductance for the transformer B is lower than it would be required for the topology. This is going to affect the modulation for this configuration and increase the power losses of the overall system.

The figure below shows the results of the overall system efficiency with each of the three transformer's configuration. With each different transformer configuration a different modulation is achieved because of the difference in leakage inductance and it will affect the overall system performance.

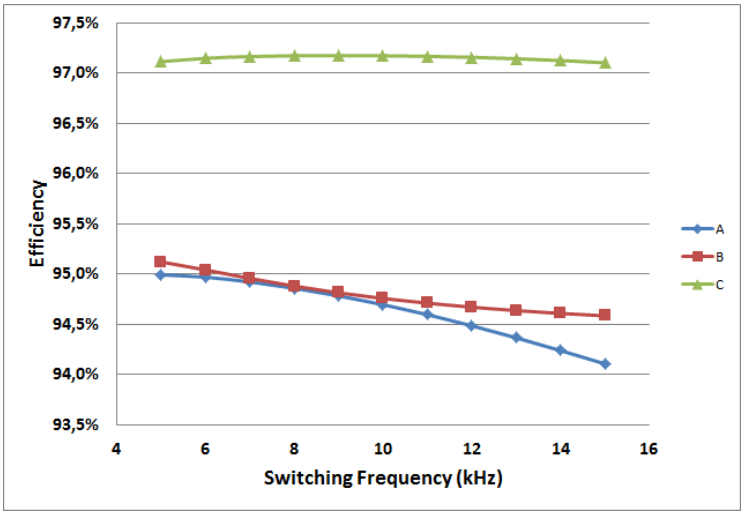

Figure 21: Efficiency vs. switching frequency for each transformer type

The transformer's configuration with best results for the efficiency is the C. Configuration A has the problem of high value for the AC resistance in the required frequency range and configuration B has a low amount of the leakage needed for this topology. The configuration C has none of this problems, it has a good amount of leakage with a minimal amount of AC resistance. For this reason it produces the highest efficiency of all the configurations.

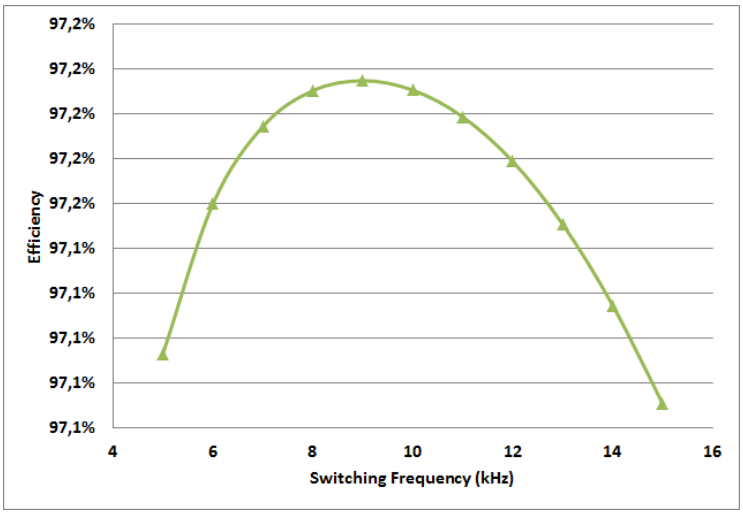

Figure 22:Efficiency of converter with type C transformer

If a closer look to the efficiency of the C configuration is taken, it can be seen that the maximum efficiency is achieved at 9 kHz

II.4.1.5 Capacitive effect in transformer design

The capacitance of the transformer should be estimated in order to ensure that the switching frequency of the converter avoids the range of the resonating frequency of the transformer. The use of copper foils can increase significantly the capacitance of the transformer.

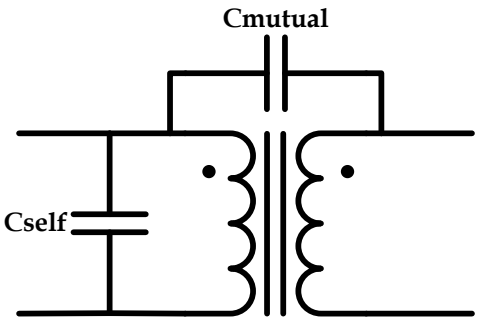

Figure 23: Capacitive effect in transformer

The result given by the finite element analysis software is the following:

Table 4
Capacitive effect of copper foils winding for the transformer

	Capacitance	Resonance
Mutual-capacitance	96 pF	8 MHz
Self-capacitance	43 pF	1.1 MHz

For the calculation of the resonance frequencies of the transformer we should take into account the resonance between the self-capacitance and the magnetizing inductance and in the other hand the resonance between the mutual capacitance and the leakage inductance.

The values of resonance are above the MHz range and they are clearly above the range of frequencies for this prototype, which is around 10kHz, so no problems should be expected for the capacitive effects.

II.4.1.6 Iteration and final result

Has the current shapes of the topology are highly influenced by the leakage inductance of the transformer and this leakage inductance is also very influenced by the position and number of turns for the windings. A process of iteration must be made in order to obtain the optimum solution for the transformer.

The number of turns is usually given by the following equation of the maximum flux density allowed.

$$n_i = \frac{\int V\,dt}{2 \cdot \Delta B \cdot A_e} \tag{13}$$

However, this equation is going to give a real number and the transformer has an integer amount of turns. Also the real turn's ratio of the transformer will be changed by the rounding effect on the number of turns.

Starting with a value of leakage inductance the current through the transformer can be simulated and then, analytically, the number of turns and losses can be estimated for the first iteration. Then it is needed to verify the results with finite element software and check if the leakage inductance is close to the value chosen. If the value is different a second iteration of simulation and calculations has to be made. The iteration must be continued until results of simulations, analytical calculations and finite element analysis are coherent with each other.

The size of the core is usually selected by the maximum flux density allowed and it also affects in the iteration process.

A summary of the final result for the design of the optimum transformer is done:

- **Copper foils:** The copper foils used for this transformer are **80 mm** wide in order to fit the core window and **0.5 mm** thick for high frequency effects. These copper foils need to be cut from a bigger sheet and wrapped with Kapton isolation. This work is done by the company Indra.
- **Primary winding:** This winding consists of **7 turns** of two sets of parallel foils.
- **Secondary winding:** This winding consists of **5 turns** of two sets of parallel pletinas.
- **Core:** The core for this transformer for this topology consists in **2 stacked cores**, **T60102-L2157-W159** of Vitroperm 500 material, from Vacuumschmelze. The cores are stacked in the f dimension.
- **Leakage inductance:** The estimation for the value of the leakage inductance is : **4 μH**

Table 5
Dimensions for T60102-L2157-W159 core

Weight	Iron cross section	Mean iron path length	Length	Width	Window length	Window width	Leg width	Height
	Afe	**lfe**	**a**	**b**	**c**	**d**	**e**	**f**
g	cm^2	cm	mm	mm	mm	mm	mm	mm
1.36	5.4	34.2	157.5	90	95	30	29.6	26.6

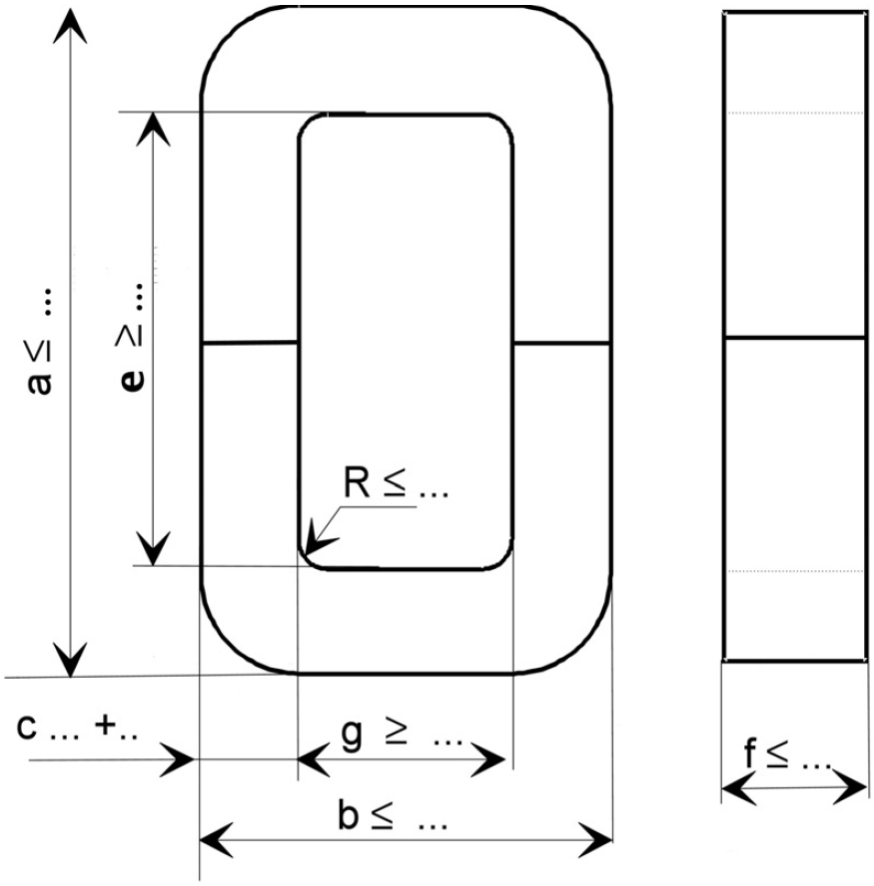

Figure 24: Limiting dimensions for 2 U-shaped halves of Vitroperm core

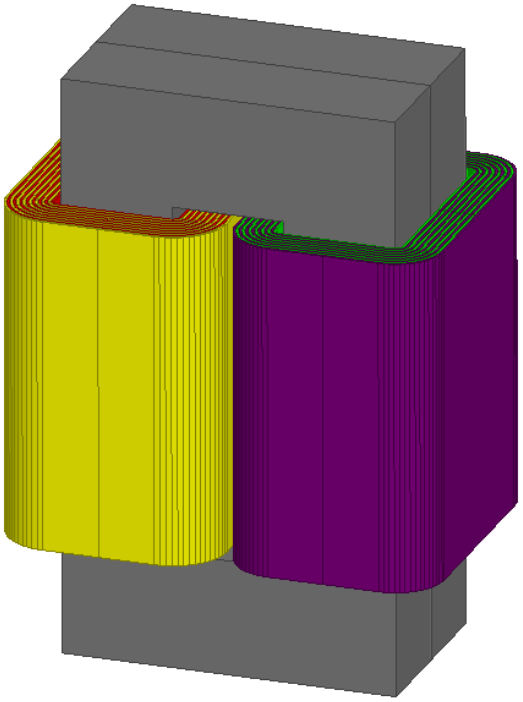

Figure 25: 3D rendering of final type C transformer

In Figure 25, a 3D rendering of the final transformer design can be appreciated. There it can also be seen the two U shape cores stacked and the windings of copper foils. This rendering is made with the finite element program MAXWELL.

III. Output capacitors

III.1 Design criteria

For the design of the output capacitors, three criteria are used:

- Maximum output ripple
- Stability of the power load at maximum load and
- Maximum voltage rise or drop in a power load step.

III.1.1.1 Output voltage ripple

The output capacitance in function of the output voltage ripple and the capacitor current is given by the following equation.

$$C_{OUT} = \frac{I_{peak}}{2 \cdot 8 \cdot f_{sw} \cdot \Delta V} = 1.04\ mF \tag{14}$$

This equation is supposing the boundary mode which would be the mode of maximum current in the capacitor. The current, in that case, is supposed to be triangular without any dead-time, so $I_{peak} = 2 \cdot I_{avg} = 2 \cdot P_{OUT}/V_{OUT} = 333\ A$. For this topology, the minimum capacitance to achieve less than 2 V of ripple at the output is 1.04 mF.

III.1.1.2 Power load stability

Considering the load as a power load the minimum amount of capacitance to have stability for a given output load is given by the following equation

$$C_{OUT} \geq \frac{1}{\pi \cdot R_{MIN} \cdot f_{BW}} = 190\ \mu F \tag{15}$$

When a load is considered a constant power load the equivalent circuit is a resistor with negative value, representing the negative slope of the constant power in a voltage vs. current plot. The equivalent circuit for this converter is shown in the following figure.

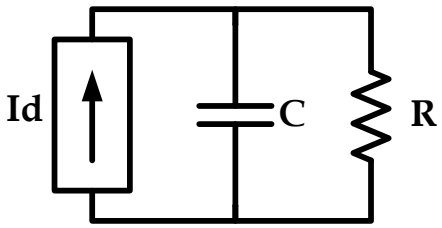

Figure 26: Equivalent circuit for power load stability criteria

This equivalent circuit has a pole in the frequency $\frac{1}{2\pi \cdot R \cdot C}$. In order for this system to be stable the bandwidth needs to be at least twice of that frequency, this criteria results in equation (15).

III.1.1.3 Power load step response

In the case of a load step in power the output voltage deviation from the steady state value is influenced by the output capacitance value. The equation that governs this behaviour is the following:

$$C_{OUT} \geq \frac{1}{2 \cdot \pi \cdot {\Delta V}/{\Delta I} \cdot f_{BW}} = 330\ \mu F \tag{16}$$

Where ΔV is the maximum voltage drop allowed and ΔI is the step up in average current. A more complex criteria is included in the Airbus regulations and its analyzed in the control and stability chapter of this work. For the design of the capacitors a increase of 150 A for the current is taken into account and a maximum voltage drop of 75 V. The bandwidth considered is 1 kHz, one decade before the switching frequency.

It can be concluded that the most restrictive criteria of the exposed before is the ripple. Subsequently the value of the minimum capacitance needed for the output of this prototype is 1mF

The capacitor chosen for this topology are 10 Epcos B32778 capacitors (of 110 µF each). The technology for this capacitors is the metalized polypropylene film, the main benefit is the highly reliability. They are also good for compact designs and have low losses are good for compact designs. They also have low losses.

III.2 Capacitor losses

The losses on the capacitor are given by the ESR of the capacitor which is usually defined in the datasheet.

$$P_{Loss\_Cap} = ESR \cdot I_{RMS\_Cap}^2 \tag{17}$$

For the output capacitors Epcos B32778 the value of ESR is 4 mΩ. But with 10 capacitors in parallel for the overall output capacitor the value of ESR is going to be 0.4 mΩ

The current of the output capacitor is shown in the figure below

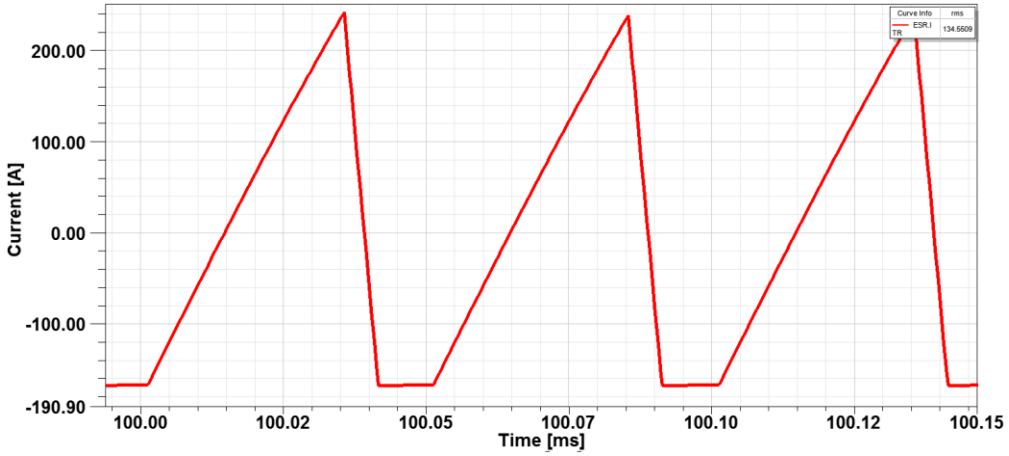

Figure 27: Output capacitor current

The real value of the RMS current for the output capacitor is going to depend on the shape of the triangular current, which is highly dependent on the leakage of the transformer, a common value of the RMS for this current is around 140A, this gives a value for the losses of $P_{Loss\_Cap} = 0.0004 \cdot 140^2 = 7.8\,W$, which is negligible in comparison to the other losses of the converter.

Optimization

As it has been seen in the design chapter, a lot of variables are depending on the final modulation for the current which in times depend highly on transformer parameters as the leakage inductance, a parasitic value not easily estimated. However it can be possible to analyze the effect of changing some open parameters in order to optimize the losses of the system. Parameters as the turn's ratio of the transformer are not in principle fixed by design.

I. IGBT hard switching minimization

The conduction losses are determined by the topology and by the output power specification. In the other hand, switching losses are also determined by the modulation of the triangular current shape, as they depend on the peak current.

There is only one non-zero current switching in a switching cycle per high-side device of each leg. The amount of energy that is lost in those transitions depends on the peak of the triangular current because the value of the DC bus voltage is constant. In order to reduce the energy loss and therefore reduce the switching losses, the modulation and the turn's ratio of the transformer can be changed to have an asymmetrical triangle and try to reduce the peak of the triangle but having the same amount of area or average current.

To reduce the value of the current peak in primary, it is needed to analyze the equation for this peak. To do that it is better to start from secondary and then use the following equation to get the primary peak current.

$$I_{PK1} = n \cdot I_{PK2} \tag{18}$$

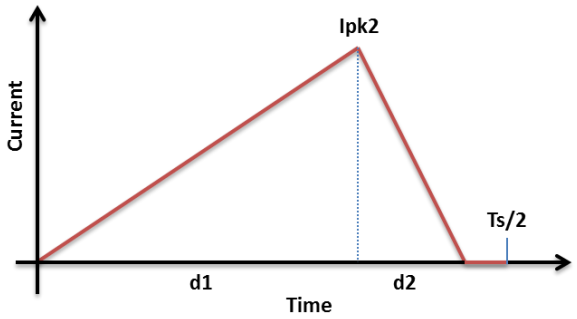

Figure 28: Primary current shape

For the maximum output power the average current in the secondary is fixed and the relation between it and the peak current in secondary is the following.

$$I_{AVG2} = (d_1 + d_2) \cdot I_{PK2} \tag{19}$$

Where d1 and d2 are given by the following equations derived from (19)

$$d_1 = \frac{I_{PK2} \cdot L_\sigma \cdot f_s}{(n \cdot V_{IN} - V_{OUT})} \tag{20}$$

$$d_2 = \frac{I_{PK2} \cdot L_\sigma \cdot f_s}{V_{OUT}} \tag{21}$$

Substituting those two equations in equation and isolating Ipk2.

$$I_{PK2} = \sqrt{\frac{P_{OUT}}{V_{IN}} \cdot \frac{(n \cdot V_{IN} - V_{OUT})}{n \cdot L_\sigma \cdot f_{sw}}} \tag{22}$$

For this equation to have a non-zero result the value inside of the square root has strictly positive. So we can derive the following relation between n, Vin and Vout.

$$(n \cdot V_{IN} - V_{OUT}) > 0 \Rightarrow n > \frac{V_{OUT}}{V_{IN}} = 0.6 \tag{23}$$

This equation is actually the buck condition modified by the transformer. This is no surprise as the full-bridge converter is a derivation of the buck converter with transformer. Finally combining this last equation with REFERENCE, the equation of the primary peak current is obtained.

$$I_{PK1} = \sqrt{\frac{P_{OUT}}{V_{IN}} \cdot \frac{n \cdot (n \cdot V_{IN} - V_{OUT})}{L_\sigma \cdot f_s}} \tag{24}$$

The values of Pout, Vin, Vout, fs and Lσ are fixed for a given value of n. It is clear that to have the minimum value for the current peak the value of n has to be also the minimum. As it is already know in equation (22), the value of n has a lower limit. So for minimizing the peak current the value of n for the transformer has to be minimized but keeping it always above 0.6. The real value of n is dependent on the rounding effect because of the integer number of turn.

Finally, this process of optimization of the turns ratio and asymmetric triangle modulation of the current as led to a decrease of losses in the hard switching of the IGBT of around 30% less losses, at a cost of increase the losses in the transformer, diodes and output capacitors, because of the high RMS values of the new modulation by only 5%, which leads to an overall improvement of the efficiency.

II. Fixed frequency vs. variable frequency control for low loads

There are two ways to control the converter at loads lower than the maximum fixed frequency of variable frequency control. In order to have the optimum efficiency for this topology in the whole range of power loads an analysis of the efficiency in those two modes has to be taken into account. The next figure shows the result of the efficiency estimation.

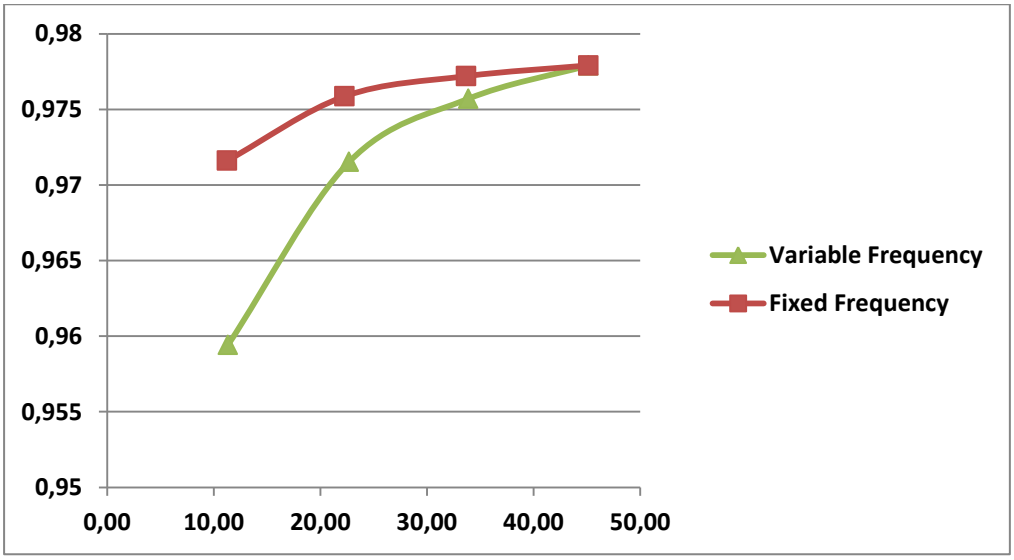

Figure 29: Efficiency of fixed frequency and variable frequency for a range of loads

It can be clearly seen that the most efficient way to control this converter is the fixed frequency, and it should be the mode chosen for the prototype. However the converter will not work properly at very low loads, so it will be needed to implement a burst mode operation for loads of less than 10kW.

Final design for the prototype

After the design and optimization process for this converter, a summary of the prototype characteristics and estimated results for losses and weight can be done:

Table 6
Final design and estimation for the prototype

Specifications	
Input voltage	**450 V**
Output voltage	**270 V**
Output power	**45 kW**
Switching frequency	**10 kHz**
Power losses	
IGBT losses	
High side conduction	96 W
High side switching	109 W
Low side conduction	120 W
Total IGBT losses	**650 W**
Transformer losses	
Copper losses (10 kHz)	134 W
Copper losses (30 kHz)	31 W
Copper losses (50 kHz)	23 W
Total copper losses	188 W
Core losses	61 W
Total transformer losses	**250 W**
Diodes losses	**410 W**
Output capacitor losses	**10 W**
Total estimated losses	**1320 W**
Estimated efficiency	**97.15 %**
Total estimated weight	**7.6**

These estimation are required to be validated in the prototype.

Control and stability

I. Control method

The control method chosen to be implemented in the prototype is the peak current mode. The advantage of this topology is that the current is controlled, which is beneficial for the implementation of protections. Also the peak current mode is necessary to have the ability to parallelize the two converters. The triangular current full bridge topology works in discontinuous conduction mode so no compensation ramp is needed in the control scheme.

For the control of this prototype a DSP is used. F28069 Piccolo controlstick from Texas instrument, this DSP has an ADC comparator output necessary for the peak current mode control

Figure 30: F28069 Piccolo controlstick from Texas instrument

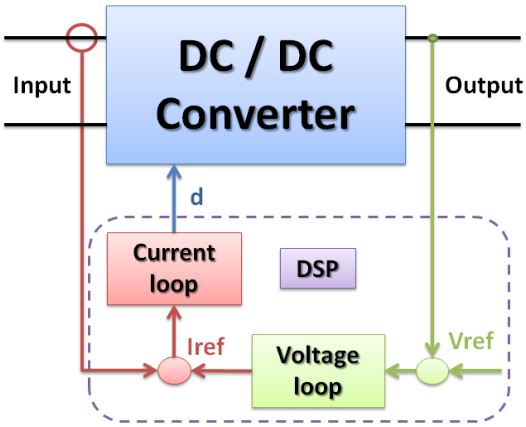

Figure 31: Control loops for the prototype

Two loops are required for this control, the peak current loop as well as the voltage loop to control the output voltage. This can be seen in Figure 31.

As the current in the leakage inductor is fixed by the topology, it stops being a state variable. The equivalent averaged circuit to control consists of two dependent current sources, modeling the primary and secondary currents of the transformer.

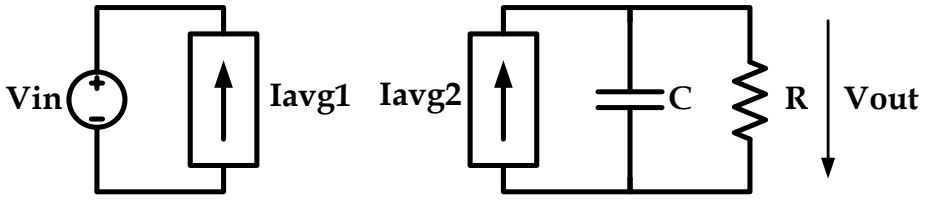

Figure 32: Triangular current equivalent circuit for averaged model

The primary averaged transformer current can be calculated with the following equation.

$$I_{AVG1} = \frac{n \cdot V_{IN}}{V_{OUT}} \cdot \frac{L_\sigma \cdot f_s \cdot I_{PK}^2}{(n \cdot V_{IN} - V_{OUT})} \tag{25}$$

The secondary averaged current, which is the output current, can be derived from equation easily with the power balance in the transformer.

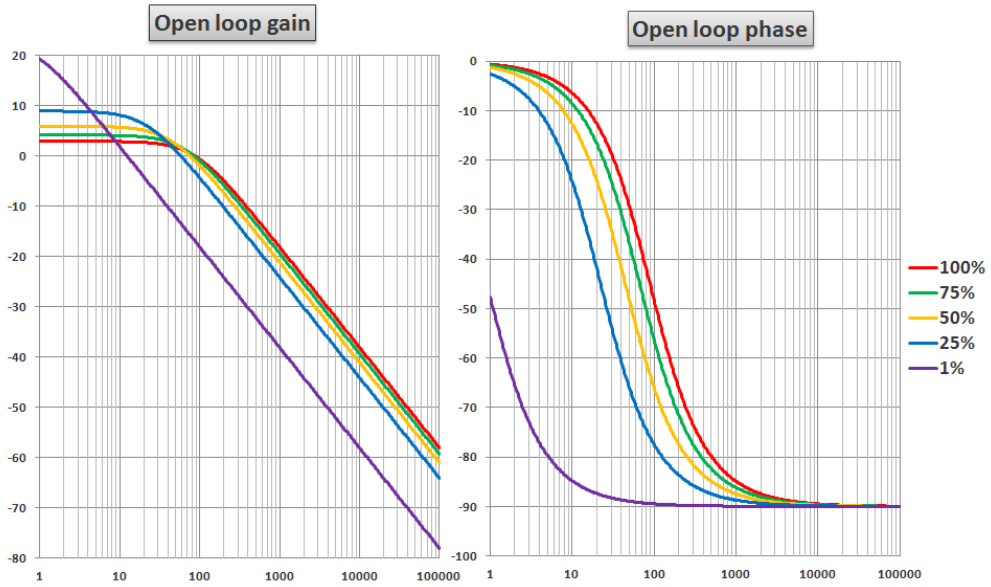

Figure 33: Open loop system Bode plot

The transfer function of the system depends on the output voltage, input voltage and current in the transformer. This transfer function is highly non-linear. In order to simulate, an approximate linearized model is made and simulations are run with the software SIMPLIS. The result of the transfer function in open loop can be seen in Figure 33. A Full range of power loads is analyzed in order to design a regulator able to deal with the pulsating load.

The loop is closed at around one decade below the switching frequency to have as much bandwidth as possible. The phase margin is verified for multiple loads in simulation. A compensator with a 62 Hz zero and a 6.2 kHz pole has been designed. We put two decades between the zero and the pole to give a boost of phase in a wide range, and reach reasonable phase margin for all the loads. The ideal value to reach for phase margin is 72º. We can see in Figure 34, that for all the load steps the phase margin is between the 70º to 80º , except for the case of very low load, 1%. This is an expected behaviour as the converter does not work without power at the output. A burst mode is needed for that case in order to have the output voltage controlled.

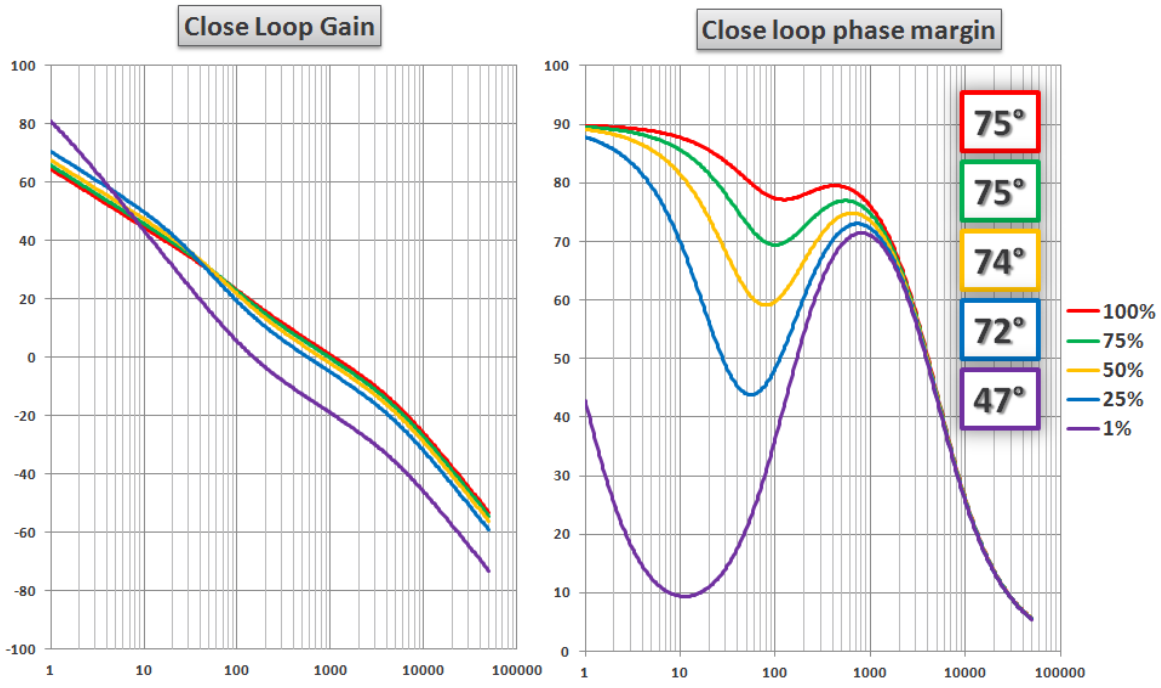

Figure 34: Closed loop system Bode plot

A summary of the phase margin per load condition can be seen in Table 7

Table 7
Phase margin for a range of output power loads

	1% Load	25% Load	50% Load	75% Load	100% Load
Phase margin	**47°**	**72°**	**74°**	**75°**	**75°**

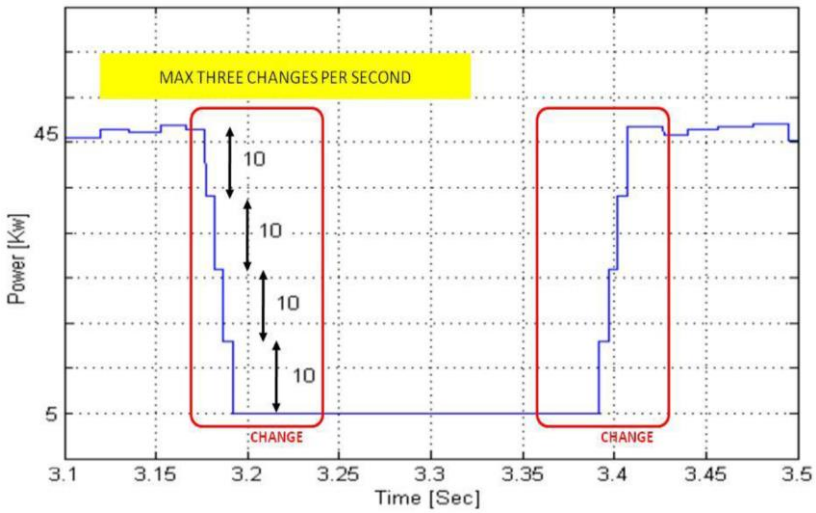

Figure 35: Load step waveform

The power step requirement consists of 4 steps of 10 kW from the maximum load 45 kW to 5 kW. During the transient that occurs as a result of this power step. The output voltage must remain in control and within the template shown in Figure 36

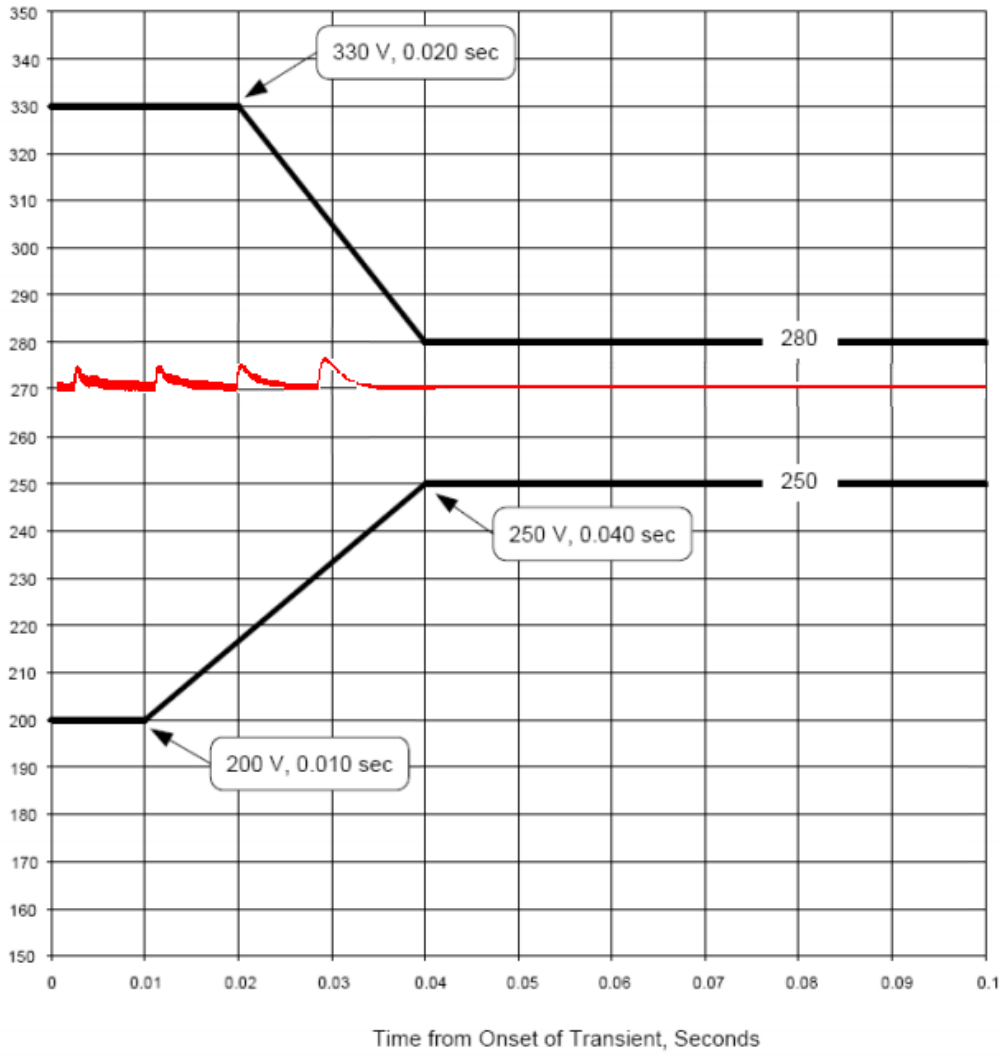

Figure 36: Dynamic template and results of transient response to load step

Simulations are run to verify the stability and dynamics of the converter defined in Figure 36. The simulation verifies the dynamic requirements. The output voltage rise is less than 6V and the recovery of the steady state. An equivalent simulation can be done for the step up in power with similar results.

II. Continuous conduction mode instability in load step condition

In the event of a load step transition, particularly a step up in power, it is possible to lose the discontinuous conduction mode for a short time during the transient. There can be instabilities if this occurs.

In the event of losing the discontinuous conduction mode, because the current has not time to reach zero in one half of the switching cycle. First the loses in the converter are going to increase because there is going to be hard switching at all the IGBT transitions. Secondly the systems equation and behaviour is changed

It is known that peak current mode control is not stable for continuous conduction mode at duty cycles higher than 0.5 without a compensation ramp. This converter doesn't have a compensation ramp because it will usually work in discontinuous conduction mode. So this explains the stability problem that can arises during transients if DCM is lost.

In order to cope with this problem, the CCM is to be avoided. This can be achieved by putting a sufficient amount of wait-time in order to make room for the triangle modulation in case of step up transients. Also an adaptive control can be made but this solution is more complex and will not be necessary if the correct amount of wait-time is implemented.

Hardware and experimental results

I. Control board and measurement boards

A control board needs to be designed to link the measurements and protections between the actual converter and the DSP. This control board consists in all the connections between the measuring signals and the DSP, along with all the filters and amplifier for conditioning the signals. It also includes all the supplies of the different voltage for the sensors and digital electronic.

I.1 Voltage measurement

The voltage measurement of the output voltage is needed in order to close the voltage loop of the system. As this voltage should be constant in steady state operation the measurement is straight forward. An instrumentation operational amplifier is used in order to boost the signal coming from a resistor voltage divider. The addition of filters can decrease the amount of noise in the measurement but this reduction of noise can also be done by software in the DSP calculation the mean value of several consecutive measurements.

I.2 Current measurement

The current measurement is the most critical in this topology. The control method is the peak current mode control. The value of the current peak needs to be compared with the reference in the DPS's ADC comparator accurately.

The value of the peak current for this topology can range between 300A and 500A. There exist current sensors of that magnitude, but usually there are bulky and heavy. For this prototype a current transformer is needed to add isolation to the current measurement, as the control board and all digital systems are grounded to the secondary side.

The current measurement consists on a current transformer, a demagnetizing circuit and an instrumentation amplifier to filter the noise a boost the signal. This current transformer is going to have a 1:500 turn's ratio. So it will need to have 500 turns. A demagnetizing circuit must be made for this current transformer in order to demagnetize in each cycle and avoid the saturation.

In order to accurately measure the peak of the current there is the need for a good noise rejection but also a good bandwidth in order to not change the shape of the current measurement.

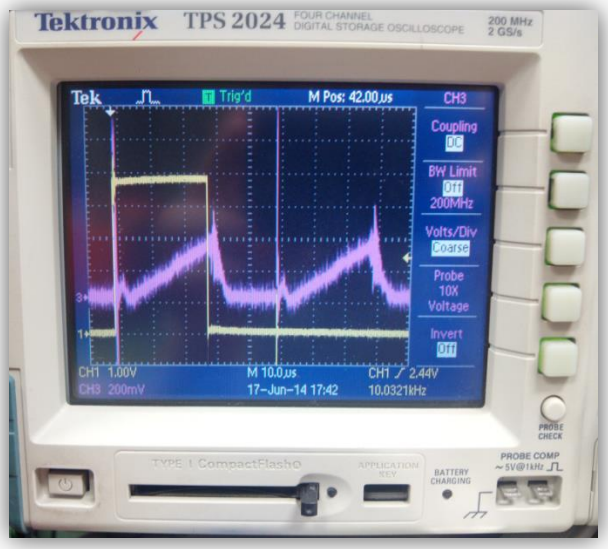

Figure 37: Current sensor voltage measured in oscilloscope.

As it can be seen in the figure above, there are some spikes at the beginning of each cycle. To avoid theses spike to affect the control and since they only appear at low duty cycles, a blanking time is added to comparator for the peak current mode in order to ignore the first 350µs.

I.3 Protections

For this prototype, protections are going to be implemented both in hardware and software for added robustness of design. The variables to be monitored are the output and input voltage; input voltage is the DC bus and also the output of the rectifier of the overall system. The input current is not actually measured but still a software protection can be implemented with the ADC comparator of the DSP. A maximum value for the peak of the current can be implemented.

I.4 Soft-start

A soft-start can be implemented by to complementary methods. The value of the maximum current peak can be increased from zero slowly as well as the maximum duty cycle allowed can be increased slowly from 0 to 50%. Additionally soft-start can also be implemented by another method. The DC bus voltage can be increased slowly by the rectifier stage.

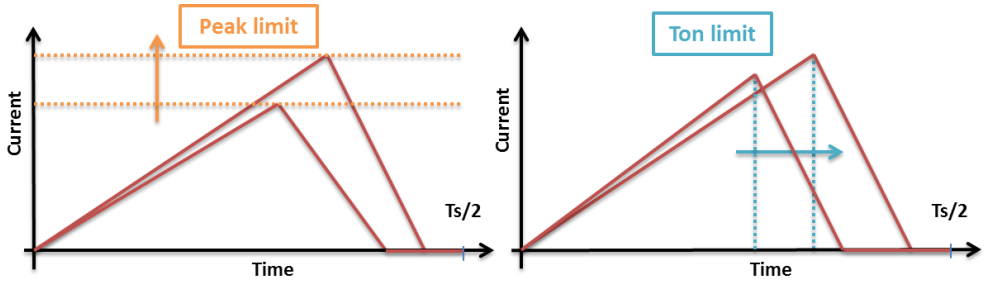

Figure 38: Soft-start methods

I.5 IGBT delays

Primary IGBT transistors are complementary to each other in one leg, which means they are alternatively on and off during the cycles. They cannot be switched both at the same time in order to ensure that the input voltage is not short-circuited.

To achieve this, a delay needs to be added to the driving signals for the IGBT. The rising from low state to high state in all of the devices should be delayed by 1µs from the falling down of the other complementary device. This value has been chosen by test on the IGBT and it still could be optimized.

II. Power stage

A prototype for this converter has been built with the help of INDRA, which designed the liquid cooling system and overall structure of the power stage. The next figure shows a 3D rendering of the prototype built by INDRA.

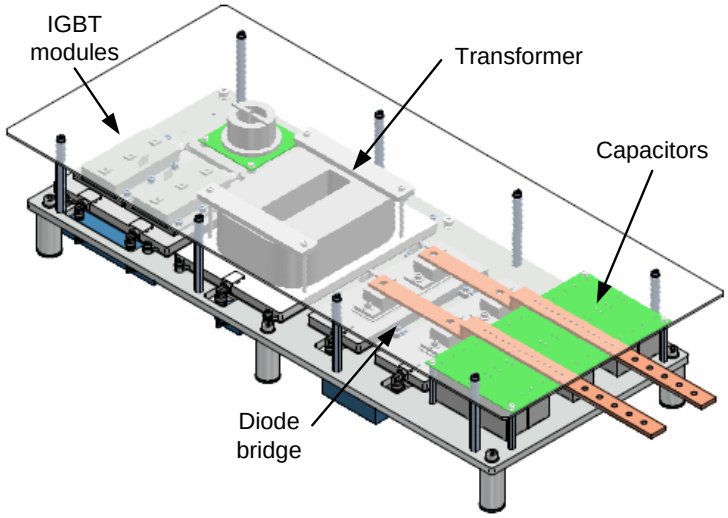

Figure 39: 3D rendering of the prototype built by Indra

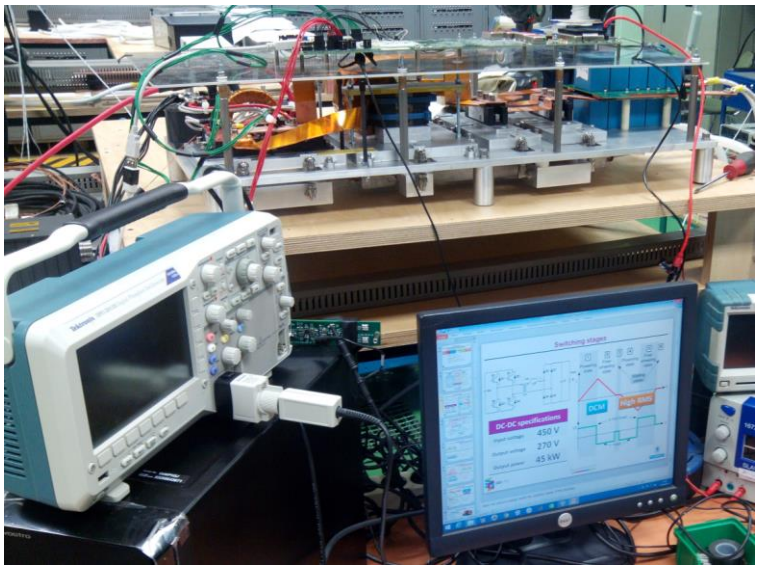

Figure 40: Workstation at Airbus

III. Experimental results

An early version of the prototype has been built with a type A transformer, before finding out of the proximity problems of that transformer configuration. The control board and software for closing the loop have been tested also. Protections and Soft-start are still being tested.

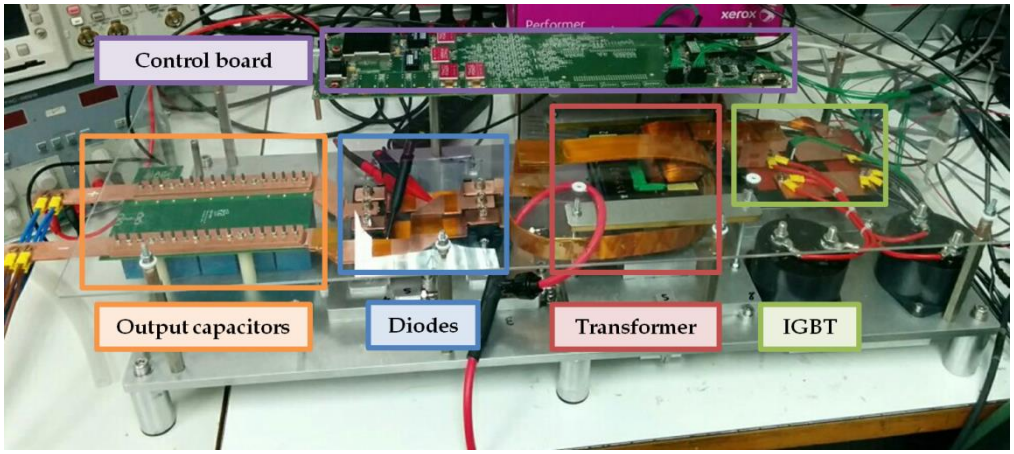

Figure 41: Prototype ready for tests at CEI laboratory

The prototype has been tested both in open loop, with only peak current and also with both voltage and current loops closed. The converter has been tested at an output power of 11 kW at a switching frequency of 10 kHz. These tests have been done with the liquid cooling working. Small transient test have been tested at that output power to check the regulator response to the transient and verify the robustness of the control.

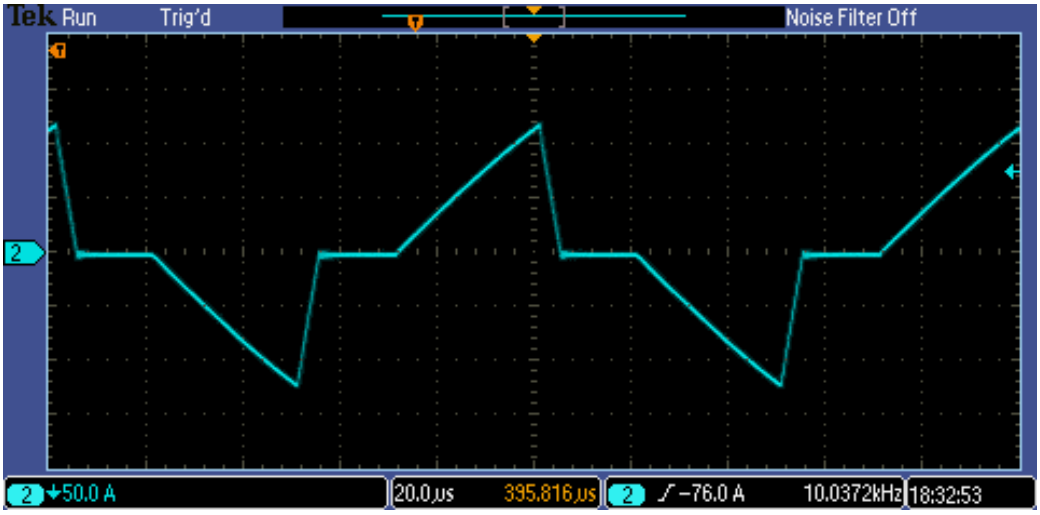

Figure 42: Primary transformer current oscilloscope capture

In Figure 42 the primary transformer current can be seen in a oscilloscope capture. The test was performed at 11kW of output power with closed loop. The triangular current shape can be seen.

It was impossible to increase the output power to levels closer to the maximum output power of 45kW because of the transformer, which is currently of type A transformer. A new type C transformer is being built by Indra to continue increasing the power and start with the test in cascade with the AC-DC rectifier.

Conclusions and future work

This Master work has been a part of the research project that was carried out in the collaboration between The Center of Industrial Electronics from The Technical University of Madrid, Indra and Airbus Defense and Space. The investigation was centered to the exploration of solutions for an airborne DC-DC converter to be included in a 45 kW rectifier.

This DC-DC converter imposes very challenging requirements. Low weight and volume must be achieved without affecting the efficiency of the system. The converter needs also to handle dynamic load steps of a pulsating load, in a stable way.

In order to cope with theses demanding specifications, the work in this project can be summarized as:

- The analysis and selection of the optimal topology for this application, looking at all of the state of the art converter topologies.
- The design and optimization of this converter. All of the components are required to meet with military standards and a derating of 30% is applied for voltage breakdowns and maximum temperatures. An optimization of the topology has been realized, minimizing the amount of switching losses by reducing the peak of the current in primary side, using an asymmetrical modulation of the current.
- Building of the prototype and tests. The prototype has being built with the help of Indra and tests have been done in CEI laboratory and are still being done in Airbus. Low power tests have been performed both in open loop and closed loop. Control boards have been designed, as well as sensor boards for all the needed measurement for the control. Liquid cooling has been also tested.

The topology is not fully validated but it has been validated at low power and both loops have been closed successfully. An optimization process has been made possible by analyzing the effects of changing the transformer turns ratio in order to have an asymmetrical modulation of the triangular current shape. Also, the effect of both control methods, fixed frequency and variable frequency, has been analyzed for the low loads conditions.

However, there is still work to do in the prototype:

- A new type C transformer is in being built by Indra. This transformer should replace the old type A transformer in the prototype to continue test.
- Tests at full power load. With the addition of the new transformer, full power tests are going to be possible in order to validate fully the topology for this application.
- Load step test from full power. The prototype should be able to handle the dynamic behaviour exposed in previous chapters. For these tests the whole range of protections are going to be needed in order to safely operate the converter and to ensure that the prototypes doesn't get damaged.
- Tests in cascade with the AC-DC rectifier in order to validate the whole system.

Finally, a part of this Master work was presented at SAAEI "Seminario anual de automatica, electrónica industrial e instrumentación", Tanger, June 2014.

Bibliography

[1] J. Biela, D. Christen, J. W. Kolar "Optimization of a 5-kW Telecom Phase-shift DC-DC converter With Magnetically Integrated Current Doubler".

[2] Z. Pavlović; J. A. Oliver; P. Alou; Ó. Garcia; J. A. Cobos "Bidirectional Dual Active Bridge Series Resonant Converter with Pulse Modulation"

[3] I.D. Jitaru " A 3kW Soft switching DC-DC converter"

[4] J.Li, T. Abdallah, and C. R. Sullivan, "Improved calculation of core loss with nonsinusoidal waveforms."

[5] K. Venkatachalam, C. R. Sullivan, T. Abdallah, and H. Tacca, "Accurate prediction of ferrite core loss with nonsinusoidal waveforms using only Steinmetz parameters."

[6] Bernardo Cougo and Johann W. Kolar, ETH Zurich "Integration of Leakage Inductance in Tape Wound Core Transformers for Dual Active Bridge Converters"

[7] "Nanocrystalline cut cores made of VITROPERM® 500 for transformers" Online: http://www.vacuumschmelze.com/fileadmin/Medienbiliothek_2010/Produkte/Kerne_und_Bauelemente/Anwendungen/Kerne/Schnittbandkerne/Cut_Cores_flyer_2011.pdf

[8] IGBT power losses calculation using the data-sheet parameters" by Dr. Dušan Graovac, Marco Pürschel, Infineon Application Note, V 1.1, January 2009

[9] Xu She, Member, IEEE, Xunwei Yu, Student Member, IEEE, FeiWang, Student Member, IEEE, and Alex Q. Huang, Fellow, IEEE "Design and Demonstration of a 3.6-kV–120-V/10-kVA Solid-State Transformer for Smart Grid Application"

[10] D. Aggeler, J. Biela, J. W. Kolar "A compact, high voltage 25kW, 50kHz DC-Dc converter based on SiC JFETs"

List of Figures